The teeth and dentition of Monacanthidae revisited tomographically

Hirofumi Kanazawa

Nihon University Graduate School of Dentistry,

Major in Anatomy

(Directors: Prof. Keitaro Isokawa and Assoc. Prof. Yosuke Yamazaki)

Table of Contents

The following article on *Stephanolepis cirrhifer* and unpublished work on *Thamnaconus modestus* and *Aluterus monoceros* are part of this doctoral dissertation:

> Hirofumi Kanazawa, Maki Yuguchi, Yosuke Yamazaki, Keitaro Isokawa (2019) The teeth and dentition of a filefish (*Stephanolepis cirrhifer*) revisited tomographically. Journal of Oral Science, in press

Abstract

The upper and lower teeth-bearing jaws in three species of the filefishes (*Stephanolepis cirrhifer, Thamnaconus modestus* and *Aluterus monoceros*) were scanned by a micro CT system, and the tooth and dentition were examined in order to address the gaps between the traditional morphology and histology. 2D tomograms, reconstructed 3D models and their virtual dissection allowed us to examine and think about the *in situ* geometry of tooth implantation and the mode of tooth attachment separately and connectedly. There were no distinct sockets comparable to those in mammals, but instead shallow depressions were observed on the premaxillary and dentary. An opening of the tooth pulp cavity was not simply directed to the seeming tooth base at an opposite direction of the tooth apex. The opening was distorted basoposteriorly or basoanteriorly depending on a position of the tooth, and the edge of pulp cavity opening was barely ankylosed; i.e., the sites of pleurodont ankylosis along the basoposterior or basoanterior edge of the opening appeared to fit nicely with the contour of a shallow depression of bone. In addition, the upper dentitions in the three species had unique morphological characteristics possibly related to their phylogenetic position. These 3D findings are undoubtedly advantageous for in-depth understanding in the phylogeny of tooth and its attachment.

Introduction

The family of the filefishes (Monacanthidae) holds 102 species in 27 genera and has a close taxonomical relationship with the triggerfishes (Balistidae) (Matsuura, 2015). These two sister families are therefore placed together in a suborder termed the Balistoidei (Tyler, 1980) in the Tetraodontiformes (Order#85 in "Fishes of the World", Nelson et al., 2016).

Owen (1840) published "Odontography" and described in detail the teeth and dentition of a grey triggerfish (*Balistes forcipatus*; synonym of *Balistes capriscus*). He compared his findings with those of a queen triggerfish (*Balistes vetula*), which had been reported in a Swedish personal communication, translated into German and filed (Retzius, 1837). They made quite precise and valuable observations in the number, morphology and some histology of the teeth and dentition of triggerfishes. Among observations on *B. capriscus*, tooth attachment interpreted as a double gomphosis was a curious issue. Indeed, Soule (1969) did report, after examining *Balistes bursa* (a synonym of *Sufflamen bursa)* and two other balistids, that the connective tissue comparable to mammalian periodontal ligament connected their teeth and bone in shallow alveolar sockets. However, the presence of a periodontal ligament has not been commonly accepted in the triggerfishes or any other actinopterygians (Berkovitz & Shellis, 2017).

In Japan, a thread-sail filefish, *Stephanolepis cirrhifer* (Kawahagi in Japanese), is one of iconic species known to be ingredient fishes served popularly as "sashimi". An early study on the teeth of *Monocanthus cirrhifer* and *Cantherines modestus* (synonyms of *S. cirrhifer* and *Thamnaconus modestus*, respectively) was carried out morphologically and histologically by Isokawa (1955). Phylogenetic interrelationships in the balistoids were examined extensively by Matsuura (1979), based on many anatomical characters including teeth-bearing jaws, which were premaxillary and dentary. He showed that the balistids and monacanthids could be clearly separated by the number of teeth and that a

larger or smaller number of teeth in the balistoids was likely to represent more primitive or advanced phylogenetic position, respectively; i.e., the former is balistids, and the latter monacanthids. Uehara & Miyoshi (1987) examined the upper jaw of *S. cirrhifer* at the ultrastructural level and advanced greatly the histological knowledge of the teeth. They showed a fibrous attachment of the tooth to bone but also made a description that "The teeth appear to attach directly to the bone at the middle region of the labial and lingual components of the teeth". These contexts indicate that, although the observations have been accumulating, uncertainties still remain in the morphology and histology of the tooth-bone interface in the filefishes, partly arising from a limitation in each of morphological and histological methods, and further the historical, or conventional, definitions and usage of terminology such as gomphosis, periodontium, alveolar socket, fibrous attachment, etc.

Therefore, it is important to employ a new methodological approach for addressing gaps in the traditional morphology and histology. Fortunately, it could be undertaken very efficiently and reliably by a present-day micro CT system (Isokawa et al, 2008; Namba et al., 2010). In addition, three-dimensional visualization would facilitate the studies on the *in situ* geometry of tooth implantation and the mode of tooth attachment separately and connectedly, which must be significant because those two aspects of tooth and its supporting tissue are not completely interdependent and thus should not be mixed (Bertin et al., 2018). The present study utilized a micro CT equipment and examined the jaw teeth and dentition (excluding pharyngeal teeth) of the filefishes, in order to compare the findings in the tomographical analyses with those in previous morphological and histological studies. Also focused was the development of (and replacement to) successional teeth.

Materials and Methods

Specimens

Three species of the filefishes (*S. cirrhifer, T.modestus and Aluterus monoceros*) approximately 24, 30 and 58 cm each in TL, were fixed with 10% buffered formalin and labeled serially as Sc#1, 2, 3 and 4, Tm#1 and 2, and Am#1 in this study. These fish collected in the Metropolitan Central Wholesale Market (Tsukiji, Tokyo) from Goto Islands, Nagasaki were obtained through a local distributor with a generous help of Professor Noriaki Koshikawa (Nihon University School of Dentistry; NUSD). Processing of the filefish was carried out in the context of a guideline by the Animal Experimentation Committee of NUSD, which is in compliance with the Nation Act on Welfare and Management of Animals.

CT Scanning and observations

Upper and lower teeth-bearing jaws were scanned by a micro-CT system (R_mCT, Rigaku, Tokyo, Japan) with the X-ray exposure of 90 kV, 100 μA, at 2×, 4×, and 6.7× magnifications and the 2-min exposure. Volume data were resliced with i-VIEW software (J. Morita, Kyoto, Japan) and exported to Dicom viewers; final isotropic voxel sizes were 100, 50 and 30 μm, respectively, in the volume data at 2×, 4×, or 6.7× magnification. Most of observations were performed utilizing multiplanar reconstruction (MPR) and 3-dimensional volume rendering (3D-VR) provided in RadiAnt DICOM Viewer (version 4.6.9 and 5.5.0; Medixant, Poznan, Poland). An another DICOM viewer, Mango (version 4.1; Research Imaging Institute, UTHSCSA, USA), was used to generate 3D-surface VR images, which were useful in examining occlusal relationship of upper and lower teeth.

A “Scalpel” tool in the RadiAnt was preferably used to extract a tooth from the 3D-VR image, or to remove the tissues other than teeth to a considerable extent. This work was aided greatly by controlling window level (WL) and window width (WW) and also

allowed to measure reliably the maximum mesiodistal width of a functional tooth (predecessor) and its successional tooth, since in doing so both measurements was done on their surfaces of interest in an identical 3D image generated in the RadiAnt.

Symbols of tooth and its position

The tooth and its position within the jaws were expressed with a symbol in this study; a tooth in outer and inner rows of the upper dentition in premaxillary was expressed as “o” and “i”, respectively, and a bowl-shaped tooth in the lower dentition in dentary was “b”, and the number following these letters indicated their order from mesial end at the mid-sagittal plane. Successional tooth was expressed in the symbol with a postfix of “s”; i.e., a successional tooth for b3 was b3s. Every erupted tooth and developing tooth identified in MPR tomograms was evaluated and scored as “calcified” or “detectable”, and the others were recorded as “undetectable (radiographically)”. This notation rule and scoring were illustrated in Figure 6.

Results

Observations in *S. cirrhifer*

The teeth observed in the upper jaw were 10 in total; 3 each (o1-3) in the right and left sides of an outer row of dentition, and 2 each (i1-2) in the right and left sides of an inner row of dentition. In the lower jaw, 6 teeth, 3 each (b1-3) in the right and left, were aligned in a single row (Fig. 1).

Labial surface of o1-3 and b1-3 was basically smooth rectangle with an obtuse apex (Fig. 1D-F). There were apparent indications of wear in the apex in some of the mesial teeth. Teeth in a row were closely aligned with each other, and a mesial pair (o1 or b1) was larger than the others except for o3, which appeared wider than o1 when examined without mucosa (Figs. 1F and 2A).

Lingual surface of i1-2 was exposed more widely over the oral mucosa (Fig. 1B). The surface consisted of a rectangular part with rounded edge at the base and a triangular part with an apex bended slightly towards labial side (Fig. 2B and C). The rectangular part had a series of perikymata-like characteristic linear grooves. The apex of triangular part in i1 and i2 was projected to gaps in o1-2 and in o2-3, respectively, and thus apical parts of outer and inner rows of upper teeth were intercalated with each other and formed a continuous dental arch cooperatively (Figs. 1B and 2A-C).

In lower dentition, there was a lingual cingulum in each of b1-3, and the developed cingulum made the lingual surface of teeth coved. The size of such shallow bowl-like concave was largely proportional to the size of the “bowl” teeth themselves (Figs. 1C, 3B and C). An array of these bowl-like concaves right behind the labial apical edge appeared to aid in durophagy in the filefishes, since this array of “bowl” was exposed entirely over the oral mucosa (Figs. 1C and 3C).

Observation of tomograms in the upper jaw (Fig. 2D-K) yielded a deeper understanding of filefish dentition. The teeth of o1-3 were observed as subtrihedral in

shape. At apex, the tooth is a solid trihedral (typically in o1, Fig. 2D-F) and all three surfaces were covered with a highly calcified tissue, which must be enameloid. When away from apex, a hollow cavity appeared (Figs. 2G-I and 4A-D), and then it changed to a groove which opened lingually and became wider towards the tooth base (facing to supporting bone) (Figs. 2J, K and 4D-F). At these levels of tomograms, the labial surface of o1-3 was wider, and its radiopaque surface layer extended towards the tooth base longer than the other two surfaces (Figs. 2F-K and 4A-E). The teeth of i1-2 were observed as a highly calcified plate-like morphology with an apical ridge (Figs. 2F-H, 4C and D), and the latter gave rise to one central and two peripheral ridges facing to bone; the radiopacity of these ridges were lower than a plate-like part (Figs. 2I-K and 4D-F).

Tomograms in the lower jaw showed that the teeth of b1-3 and their successors were trihedral. The solid apex and the transition of pulp cavity from tubular to groove-like were also observed in b1-3, and the enameloid did cover b1-3 (Fig. 3D-K) basically in a similar fashion observed in o1-3. In addition, the surfaces of lingual bowl-like concaves in b1-3 and in their successors were surely covered with a radiopaque layer of enameloid (Figs. 3L-Q and 4H-J).

Tomograms at a higher magnification revealed the link between functioning teeth and their supporting bone. The bone did not come up close to the apices of all three types (o, i, b) of functioning teeth. In the upper jaw, the teeth of o1-3 and i1-2 were ankylosed barely to the supporting bone at the tooth base and/or at the basal one third in the ridges facing to the bone (Fig. 4A and F). In the lower jaw, the teeth of b1-3 were again ankylosed faintly to the bone at the tooth base (Fig. 4H-J). In contrast, no bony ankylosis was found in the developing successional teeth.

The successional teeth were being developed beneath the functioning predecessors. The erupted teeth and their successors were aligned almost coaxially, but such axis of o3-o3s was considerably tilted distally compared to those of o1-o1s and o2-o2s (Fig. 5A and B). The width of successional teeth measured in this study was approximately 10% larger

than their predecessor teeth (Table 1), though these successors might develop further before their eruption.

The development of successional teeth was asynchronous. They were varied in size and in tomographical signal intensity, and thus multiple tomograms were needed to be examined closely in order to trace developing successors. In addition, some of developing teeth detectable in tomograms could not be shown in a 3D-VR image (e.g., right i2s of Sc#3 in Figs. 5A and 6). In this study, while only one tooth (left o1 in Sc#3) had been exfoliated among 64 functioning teeth in four samples of *S. cirrhifer* (Sc#1-4 in Fig.6), and the number of successors evaluated as "calcified", "detectable" and "undetectable (radiographically)" was 41, 7 and 16, respectively, in *S. cirrhifer*. Distribution of successors in these three developmental categories was illustrated in a recording chart (Fig. 6).

Observations of individual teeth extracted digitally from the 3D-VR were very informative. Transition of pulp cavity from tubular to groove-like images in o1-2 (Fig. 4D-F) could be understood in depth by knowing their 3D morphology. Indeed, the changes of the number of labial ridges in i1-2 and i1s in tomograms (Fig. 4C-G) became easily accountable with Figure 5E and F. More importantly, it turned out that pulp cavity was not simply open at the seeming tooth base but elongated and open widely to a basoposterior direction in o1and o1s (Fig. 5C and D) and to a basoanterior direction in i1 and i1s (Fig. 5E and F), and thus the lingual ridges in o1 and labial ridges in i1 were actually a part of the edges of a pulp cavity opening. About a half or basal two thirds of the edge of cavity opening, was sites of ankylosis between tooth and its supporting bone (arrowheads in Fig. 5C and E). That part of the cavity opening was sitting on the bony shallow depressions (Fig. 5G and H).

A wear of apex in functional tooth was evident by comparing it with an apex of the unerupted successor (compare Fig. 5C and D); in addition, a worn apex was indented at the tip, indicating difference in the hardness of outer enameloid and inner dentin (see

"apical aspect" in Fig. 5C). Differences of basal aspects in Figure 5C and D indicated that an increase of dentin thickness was still in progress in the successor (Fig. 5D). Moreover, the perikymata-like linear grooves had been developed already in the lingual surface of an unerupted successor (i1s in Fig. 5F), in which the bone-side morphology was still incomplete compared to that of the erupted tooth (compare Fig. 5E and F).

The occlusion of upper and lower teeth was well delineated by 3D-surface VR images (Fig. 7). When the jaws were closed, the apex and its distal nipping edge of b1 contacted closely with the lingual surface of i1, but not with o1. Similarly, b2 contacted with both i1and i2, and b3 contacted with i2. Thus, there was an arch-shaped contact between i1-2 and b1-3 dentitions. In just behind the arch-shaped contact, mucosal membrane of the oral cavity was protected with hard tissue armors; i.e., a roof provided by four inner teeth in the above and a basal terrace made of an array of bowl-like concaves in the lower dentition.

Observations in *T. modestus and A. monoceros*

The number and a position of teeth observed in these two species were identical to those observed in *S. cirrhifer*: namely, 10 teeth in the upper and 6 teeth in the lower jaws, and there were an outer and an inner dentition (consisting of o1-3 and i1-2, respectively) in each of left and right upper jaws (Fig. 8). Therefore, the same symbols and chart could be used for recording of the tooth development in these species (Fig. 6).

Overall morphology of the tooth in *T. modestus and A. monoceros* (Fig. 8) was similar to that in the same position in *S. cirrhifer* (Fig. 1), but all of the most mesial teeth (o1, i1 and b1) in *A. monoceros* were slender than o2, i2 and b2, respectively. In *T. modestus*, b1 was larger than b2 in width, and o1 and i1 was slender than o2 and i2. The latter, however, might just represent the asynchronous tooth replacement.

Perikymata-like linear grooves in the lingual surface of i1-2 were observed clearly in *T. modestus*, but less discernible in *A. monoceros*, while the lingual surface of i1-2 in

both species was exposed widely over the oral mucosa and appeared to provide a hard tissue roof just behind the upper dental arch (Fig. 8C, F). It was also true in the lower dentition that there was a well-developed lingual cingulum in each of b1-3, which appeared to provide a basal terrace made of an array of bowl-like concaves of b1-3 teeth. The edges of bowl-like concaves in b1-3 appeared to be very sharp in *A. monoceros*, compared to the other two species.

As in the case of *S. cirrhifer* (Figs. 1B and 2A-C), the apex and a part of nipping edge of i1-2 and o1-3 were intercalated with each other and formed a continuous dental arch cooperatively. However, their labial and lingual aspects showed a characteristic difference among the three species examined in this study (Fig. 9). In *S. cirrhifer*, the apex of i1 and i2 was projected to the gaps in o1-2 and in o2-3, respectively (Figs. 1B, 2A-C and 9A, B). On the other hand, i1-2 teeth in *A. monoceros* somewhat resemble the Gingko leaf (biloba, or bifid-shape) and possessed a notch in their nipping edge (Fig. 9F), and the notch was positioned perfectly to fill the gaps between o1-2 and o2-3 (Fig. 9E) in the intercalation of the outer and the inner teeth. It was really curious that i1 and i2 teeth in *T. modestus* possessed an apex and a notch, respectively. The apex was projected to the gap in o1-2 and a notch fill the gap in o2-3 (Fig. 9C, D). It would be noteworthy that the developing successors of bifid-shaped inner teeth possessed also a notch in their nipping edge.

Since the tomographical tooth morphology in *T. modestus* and *A. monoceros* was basically similar to that in *S. cirrhifer*, their details were not given here, but representative tomograms demonstrating the geometry of tooth implantation and the mode of tooth attachment were shown in Figure 10. Geometrically, all of o1-3, i1-2 and b1-3 were pleurodont, and those were attached to the shallow depression of bone with ankylosis (see insets of Fig. 10). Ankylosis was appeared to occur at the edge of pulp cavity opening which was distorted basoposteriorly or basoanteriorly depending on a position of the tooth. There was no socket for the teeth in all three species of the filefishes examined in this

study.

In the developing successional teeth, their width was approximately 10% larger than the predecessor teeth (Tables 2 and 3), and no ankylosis to the bone was found (Fig. 10).

Discussion

It was shown in this study that the highly elaborate morphologies of the tooth and dentition of the filefishes could be investigated in greater detail using a present-day micro CT system. Some of the present findings were reported already by Isokawa (1955), Matsuura (1979) and Uehara & Miyoshi (1987) through their perceptive observations and efforts in the morphological and histological approaches. However, the present study conducted with 2D tomograms and reconstructed 3D models can be undoubtedly advantageous, even though the histological works at the light and electron microscopic levels need to take part in an inevitable aspect of the studies for tooth morphology.

Since the analyses of dataset generated by micro CT allow non-destructive observations, the teeth with *in vivo* geometry in the specimens could be interrogated serially back and forth and as 3D models from various directions, resulting in identification of all of the functioning and their successional teeth *in situ*. In addition, "virtual dissection" described as "extracted digitally from the 3D-VR" was possible with a scalpel tool (Figs. 5, 10). This approach met with a plenty of valuable findings, which were also beneficial to understand in depth the tomographic images. A smallest voxel size in original images presented in this study was 30 μm^3; which was feasible for evaluating the link between the teeth and bone (Figs. 4, 10) and for measuring the width of developing teeth *in situ* in the 3D models (Tables 1-3). Kazzazi & Kranioti (2018) reported that measurements on 3D-VR images were accurate and reliable in comparison with traditional odontometrics carried out on real teeth with digital calipers.

The mode of tooth attachment in balistoids has been controversial for a long time. Owen (1840) described it as a "double gomphosis" in *B. capriscus*, but it appeared to imply that the teeth were implanted in bony sockets, while bony struts projecting from alveolar bone were implanted in the narrow spaces between teeth. Isokawa (1955) reported that the teeth in *S. cirrhifer* were ankylosed barely on the bone margin via

predentin. Soule (1969) reported on *S. bursa* and two other balistids that the tooth attachment was composed of a shallow alveolar "socket", a "periodontal" ligament and acellular "cementum". Berkovitz & Shellis (2017) appeared to be unconvinced by the latter results and agree more with the attachment by ankylosis to shallow bony depressions. Uehara & Miyoshi (1987) showed that the upper teeth of *S. cirrhifer* were tightly fixed to the jawbone by bundles of fibrils and also that the teeth appeared to attach directly to the bone at the middle region of the labial and lingual components of the teeth. In the present study, the tooth shape and related geometry have been examined and visualized three-dimensionally in jaws of *S. cirrhifer*, *T. modestus* and *A. monoceros*, and thus this author could note confidently here that there were no distinct sockets comparable to those in mammals, and that the edge of pulp cavity opening was ankylosed barely to the bone depression (arrowheads in Figs. 4, 5, 8 and 10).

It was again observations of the 3D-VR that resolved the uncertainty how the filefish teeth were ankylosed to shallow depressions of bone. An opening of the tooth pulp cavity was not simply directed to the seeming tooth base at an opposite direction of the tooth apex. The opening was distorted basoposteriorly in o1-3 and b1-3, and basoanteriorly in i1-2, and therefore a part of the basoposterior or basoanterior edge of the opening was ankylosed to the bone (Figs. 4, 5C, E and 10); it means that the tooth was pleurodont, but not ankylosed to the bone by means of their actual labial or lingual walls. Pleurodont is a mode in which the labial (or lingual) surface of the tooth is set against the labial (or lingual) side of the tooth-bearing bone. The distribution of such pleurodont ankylosis along the edge of the pulp cavity opening appeared to fit nicely with the contour of a shallow depression of the supporting bone (Figs. 5G, H and 10).

The presence was reported of a periodontal ligament and cementum as the attachment apparatus for the teeth of balistids (Soule, 1969), but these two tissues were considered to be peculiar in Crocodilia and Mammalia (Berkovitz & Shellis, 2017), hence being non-existent in almost all Osteichthyes. Indeed, Isokawa (1955) reported that there

was nothing which was called the cementum, but that the “predentin” was found in the boundary area of teeth and bone of *S. cirrhifer* and *T. modestus*. This statement was confirmed by re-examinations of the histological specimens he had prepared in the early 1950s (Kanazawa et al., 2019). The latter authors have also noted that the predentin or its equivalents extended to the outer surface of the edge of pulp cavity opening, and that it could be an anchorage for fibers connecting tooth-to-bone and tooth-to-tooth. These two types of fibers were also reported in an electron microscopical study by Uehara & Miyoshi (1987). The tooth-to-tooth fibers should not be described as “periodontal”, and the tooth-to-bone fibers were considered as a part of “fibrous attachment”, which is relatively common in Osteichthyes (Fink, 1981). Therefore, it is plausible that the fibrous attachment coexists with ankylosis and reinforces the tooth attachment in the filefishes.

The surface rendering in this study showed how the upper and lower teeth of *S. cirrhifer* meet together (Fig. 7); i.e., the continuous arch consisting of the apex and its distal nipping edge of b1-3 came in contact completely with the lingual surface of i1-2. Since the dentary is articulated with quadrate, and the maxillary and premaxillary are articulated with palatine, the upper and lower jaws could both rotate in the species of this family (Matsuura, 1979; Konstantinidis & Johnson, 2012). Thus, the flat and wide lingual surfaces of teeth i1-2 (Fig. 7) would serve as a cutting or crashing board after pecking and capturing prey. Feeding habits of the filefishes could vary from herbivorous to carnivorous, with many being omnivorous (Matsuura, 1979; Tyler, 1980; Akagawa & Okiyama, 1997). The stomach contents of *S. cirrhifer* caught in the southern Shikoku, Japan were reported to have had amphipods, barnacles and sea urchins (Kawase & Nakazono, 1996), most of which should include hard shells and/or calcified structures. Thus, the four inner teeth as well as an array of bowl-like concaves in the lower dentition,

both being covered with the enameloid tissue, might be functionally relevant as an armor for protecting mucosal membrane in biting the prey.

All three species of the filefishes examined in this study had the same number of teeth, and this characteristic is one of traits which could distinguish the filefishes from the triggerfishes (Matsuura, 1979). In contrast, their labial and lingual aspects of the upper dental arch showed a minute but distinct difference in the intercalation between o1-3 and i1-2 teeth among the three species (Fig. 9). These three species belong to different clades in the filefish family when assessed by the structures of pelvic complexes (Matsuura, 1979), whole mitochondrial genome sequences (Yamanoue et al, 2009; Yamanoue, 2015) and BMP gene sequences (McCord & Westneat, 2016). Therefore, the morphology (i.e., apex- or notch-type) of two inner teeth in the upper jaw is likely to represent phylogenetic divergence, possibly useful as a taxonomic character.

Conclusions

The tooth and dentition of the filefishes (*S. cirrhifer, T. modestus* and *A. monoceros*) were examined with 2D tomograms, reconstructed 3D models and their virtual dissection, in order to address the gaps between the traditional morphology and histology. The major findings drawn were as follows:

1. There were no distinct sockets comparable to those in mammals, and the edge of pulp cavity opening was ankylosed barely to a shallow depression on the bone.
2. An opening of the tooth pulp cavity was not simply directed to the seeming tooth base but distorted basoposteriorly in o1-3 and b1-3 and basoanteriorly in i1-2, and therefore teeth were pleurodont in the geometrical aspects.
3. There were an apex-type and a notch-type inner tooth. Both i1 and i2 in *A. monoceros*, only i2 in *T. modestus* and none in *S. cirrhifer were* notch-type, resulting in the species-specific appearance of the upper dentition, which was formed by intercalation of the outer and the inner teeth.

These findings have resolved a long-lasting controversial issue on the tooth attachment in the filefishes and also showed the phylogenetic divergence of inner teeth, possibly useful as a taxonomic character in the filefishes. Tomographic studies are undoubtedly advantageous for in-depth understanding of tooth morphology and its development, even though the histological works at the light and electron microscopic levels take part in an inevitable aspect of the studies for tooth morphology.

Acknowledgements

I am grateful to Prof. Keitaro Isokawa and Assoc. Prof. Yosuke Yamazaki for their valuable suggestions and critical reading, and to all the colleagues in Department of Anatomy for their technical assistance and continuous encouragement.

Literature Cited

Akagawa I, Okiyama M (1997) Reproductive and feeding ecology of *Rudarius ercodes* in different environments. Ichthyol Res 44, 82-88.

Berkovitz B, Shellis P (2017) The teeth of non-mammalian vertebrates. Elsevier Inc., London.

Bertin TJC, Thivichon-Prince B, LeBlanc ARH, Caldwell MW, Viriot L (2018) Current perspectives on tooth implantation, attachment, and replacement in Amniota. Front Physiol 9, 1630.

Fink WL (1981) Ontogeny and phylogeny of tooth attachment modes in actinopterygian fishes. J Morphol 167, 167-184.

Isokawa K, Yuguchi M, Nagai H (2008) Oxytalan fibers in the teleostean tooth and pedestal bone. Matrix Biol, 27, S22. (Abstract)

Isokawa, S (1955) Morphological studies of teeth of fishes. IV Teeth of file-fishes, Zool Mag 64, 194-197.

Kanazawa H, Yuguchi M, Yamazaki Y, Isokawa K (2019) The teeth and dentition of a filefish (*Stephanolepis cirrhifer*) revisited tomographically. J Oral Sci. (in press)

Kawase H, Nakazono A (1996) Two alternative female tactics in the polygynous mating system of the threadsail filefish, *Stephanolepis cirrhifer* (Monacanthidae). Ichthyol Res 43, 315-323.

Kazzazi SM, Kranioti EF (2018) Applicability of 3D-dental reconstruction in cervical odontometrics. Am J Phys Anthropol 165, 370-377.

Konstantinidis P, Johnson GD (2012) Ontogeny of the jaw apparatus and suspensorium of the Tetraodontiformes. Acta Zool 93, 351-366.

Matsuura K (1979) Phylogeny of the superfamily Balistoidea (Pisces: Tetraodontiformes). Mem Fac Fish Hokkaido Univ 26, 49-169.

Matsuura K (2015) Taxonomy and systematics of tetraodontiform fishes: a review focusing primarily on progress in the period from 1980 to 2014. Ichthyol Res 62, 72-113.

McCord CL, Westneat MW (2016) Phylogenetic relationships and the evolution of BMP4 in triggerfishes and filefishes (Balistoidea). Mol Phylogenet Evol 94, 397-409.

Namba Y, Yamazaki Y, Yuguchi M, Kameoka S, Usami S, Honda K, Isokawa K (2010) Development of the tarsometatarsal skeleton by the lateral fusion of three cylindrical periosteal bones in the chick embryo (*Gallus gallus*). Anat Rec 293, 1527-1535.

Nelson JS, Grande TC, Wilson, MVH (2016) Fishes of the world, 5th ed. John Wiley & Sons, Inc., Hoboken, New Jersey.

Owen R (1840) Odontography; or, a treatise on the comparative anatomy of the teeth; their physiological relations, mode of development, and microscopic structure, in the vertebrate animals. Hippolyte Baillière Publisher, London, 82-85.

Retzius A (1837) Bemerkungen über den innern Bau de Zähne, mit besonderer Rücksicht auf den in Zahnknochen vorkommenden Rührenbau, von A. Retzius. Arch Anat Physiol wiss Med 1837, 486–566.

Soule JD (1969) Tooth attachment by means of a periodontium in the trigger-fish (*Balistidae*). J Morphol 127, 1-5.

Tyler JC (1980) Osteology, phylogeny, and higher classification of the fishes of the order Plectognathi (Tetraodontiformes). NOAA Tech Rep NMFS Circular 434, 1-422.

Uehara K, Miyoshi S (1987) Structure of the upper teeth of the filefish, *Stephanolepis cirrhifer*. Anat Rec 217, 16-22.

Yamanoue Y, Miya M, Matsuura K, Sakai H, Katoh M, Nishida M (2009) Unique patterns of pelvic fin evolution: A case study of balistoid fishes (Pisces: Tetraodontiformes) based on whole mitochondrial genome sequences. Mol Phylogenet Evol 50, 179-189.

Yamanoue Y (2015) Diversity, phylogeny and taxonomy of tetraodontiform fishes. TAXA 39, 1-16.

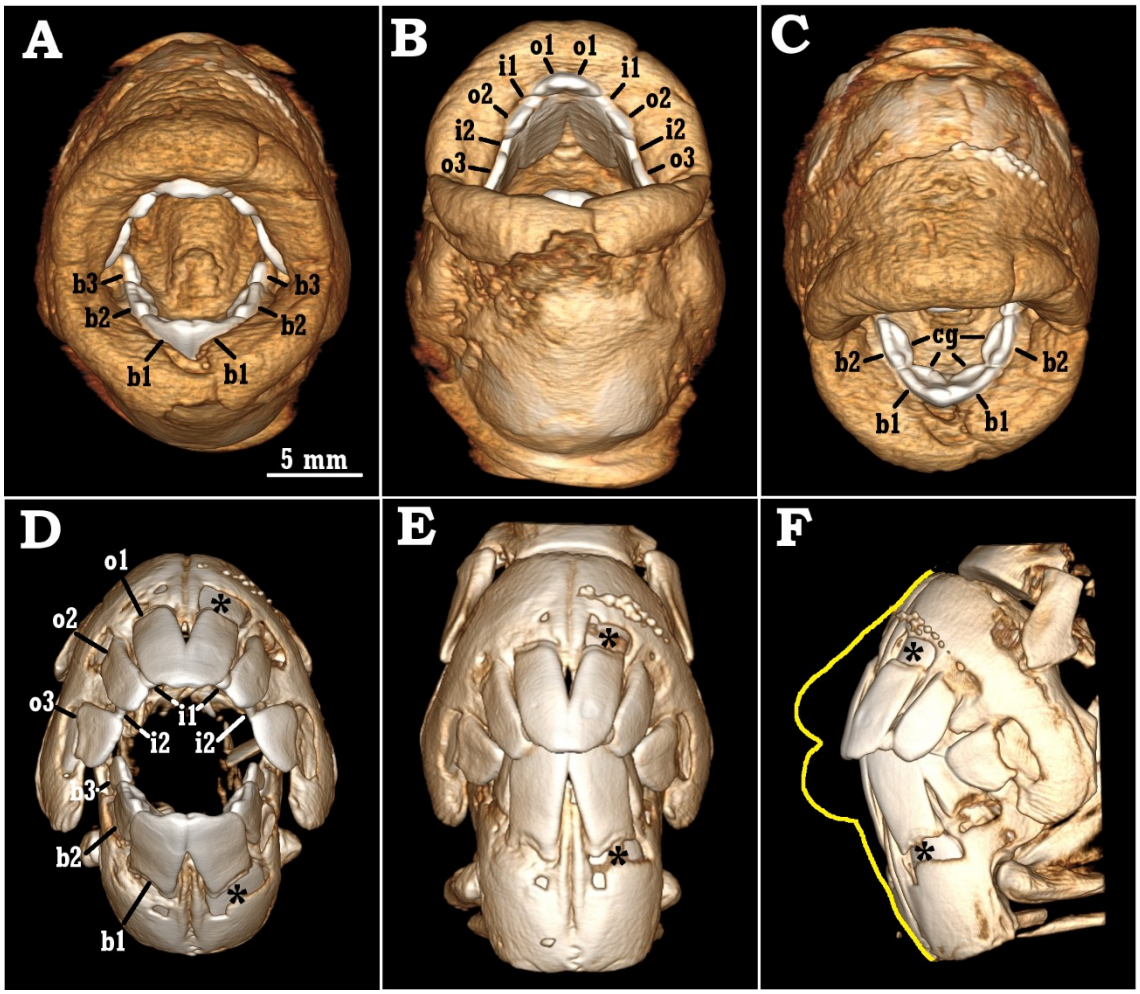

Fig. 1. The teeth-bearing jaws of *S. cirrhifer* (Sc#1) with (A-C) and without (D-F) mucosal integument.

The frontal (A-E) and lateral views (F) of the 3D-VR are shown in the open (A-D) and closed (E, F) positions of jaws; upper and lower dentitions are better demonstrated by tilting a VR image slightly upward and downward in B and C, respectively. An outline of the surface of integument is superimposed in yellow in F. Concerning symbols for tooth and its position, consult "Materials and Methods" and Figure 6. Lingual cingulum (cg) is shown in each of b1 and b2 teeth in C. Asterisks indicate successional teeth. All images are in the same magnification.

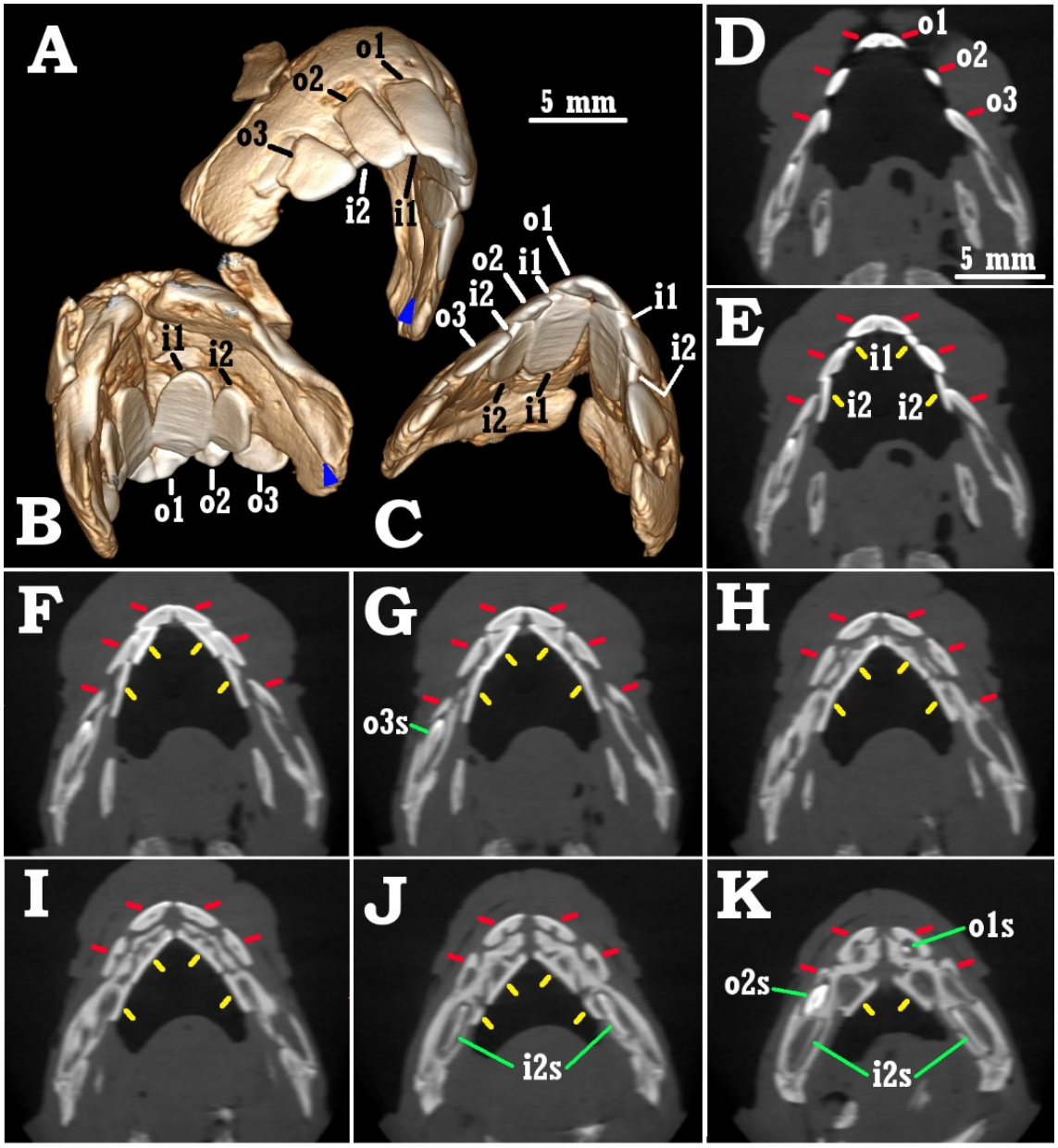

Fig. 2. The upper jaw of *S. cirrhifer* (Sc#1) viewed in 3D-VR from different directions (A-C) and in horizontal tomograms of upper dental arch in MPR (D-K).

Arrowheads in A and B indicate a fusion line between maxillary and teeth-bearing premaxillary. Tomograms are shown intermittently from the apices of o1 (D) to the deeper where the bone between outer and inner row of teeth (H-J) and some of successional teeth (J, K) could be observable. All images in D-K are in the same magnification.

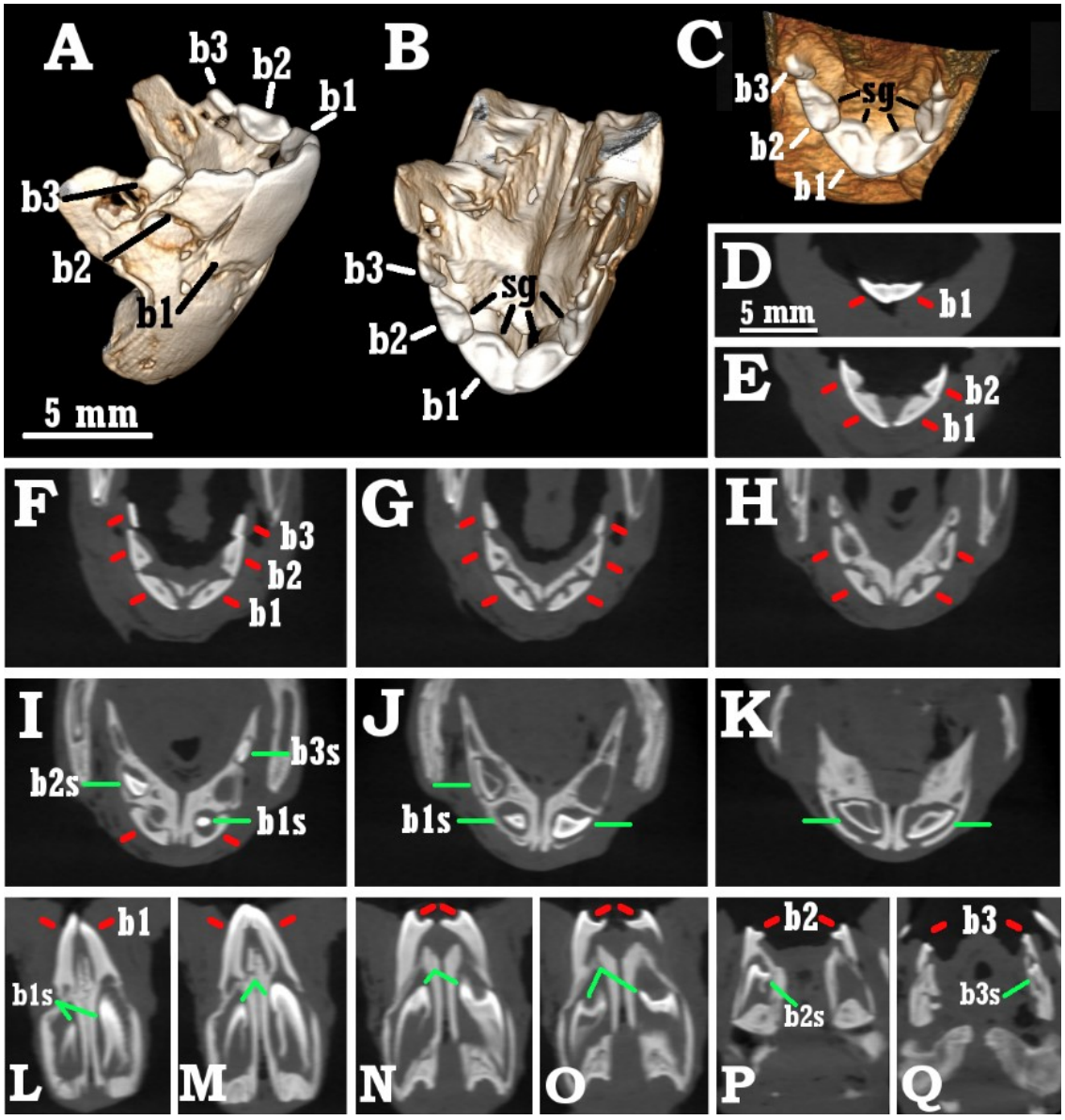

Fig. 3. The lower jaw of *S. cirrhifer* (Sc#1) viewed in 3D-VR from different directions (A-C), in horizontal (D-K) and in axial (L-Q) tomograms of lower dental arch in MPR.

Horizontal tomograms are shown intermittently from the apices of b1 (D) to the deeper where the supporting bone (F-H) and some of successional teeth (I-K) could be observable. Axial tomograms are shown intermittently from rostral (L) to caudal (Q). All images in D-Q are in the same magnification.

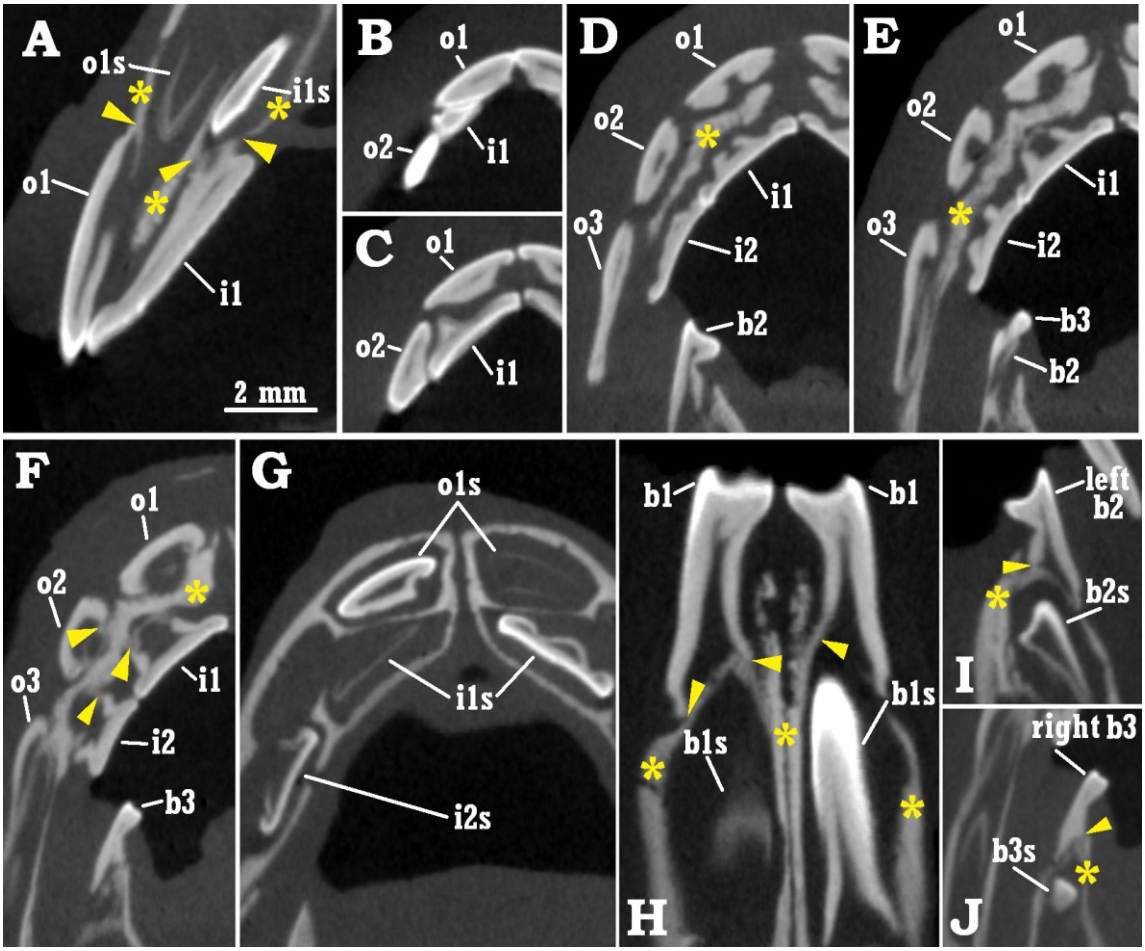

Fig. 4. Closer tomographical views of the jaws in *S. cirrhifer* (Sc#4).

A parasagittal tomogram of the left upper jaw (A), horizontal tomograms of the right upper jaw (B-G) and axial tomograms of the lower jaw (H-J) were shown at a higher magnification. Higher calcification in enameloid is better delineated. Asterisks indicate supporting bone between the o1-3 and the i1-2 (A, D-F) and in the base of b1-3 (H-J). Arrowheads point to sites of ankylosis between tooth and its supporting bone. All images are in the same magnification.

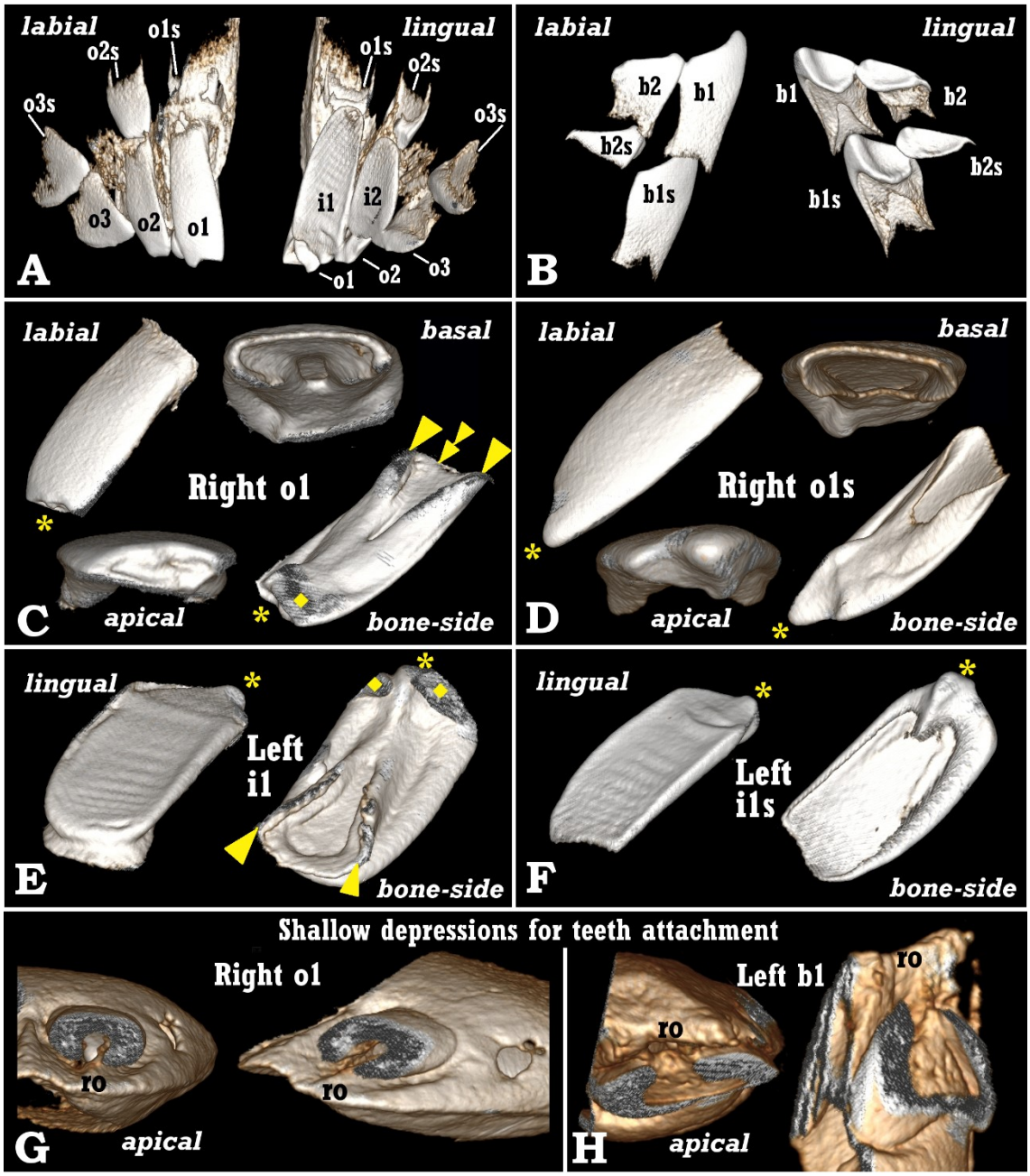

Fig. 5. The functional teeth (predecessors), their successors and shallow depressions for teeth attachment in *S. cirrhifer*.

Most of the tissues other than teeth are removed from a 3D-VR image (A-F). The o1-3 and their successors in Sc#3 are shown in the labial aspect, and i1-2 in the lingual aspect (A); no successors for i1-2 were found in this 3D-VR image. The b1-2 and their successors in Sc#3 are shown in the labial and lingual aspects (B); since this specimen lacked b3s, antecedent b3 is not included in this VR image.

(Legend of Fig. 5 continued)

(Legend of Fig. 5 continued)

In addition, o1 (C) and o1s (D) in the right upper jaw and i1(E) and i1s (F) in the left upper jaw in Sc#4 are shown individually in different four or two aspects. Asterisks indicate the apical side of individual tooth. The basal edge of o1 (double arrowheads in C) and the basal one third on the ridges of o1 and i1 (arrowheads in C and E) are both a part of the pulp cavity opening and represent a detached surface which had been ankylosed to the bone. When a tooth was extracted digitally, rough surfaces were inevitably generated (diamonds in C and E) due to the close interdigitation of apices of o1 and i1.

Shallow depressions of bone (G, H), on which o1 in Sc#3 (G) and b1 in Sc#4 (H) rested, are shown. About three- to four-fifths of the teeth are removed and the remaining U-shaped stumps sitting on the depressions are shown. The ridge of supporting bone (ro) is protruding in the lingual side of o1 and b1. Images in the right are slightly tilted towards distal (G) or shown in the mesial aspect (H). In this figure, images are varied in size, since each of them are enlarged arbitrarily to show their details as much as possible.

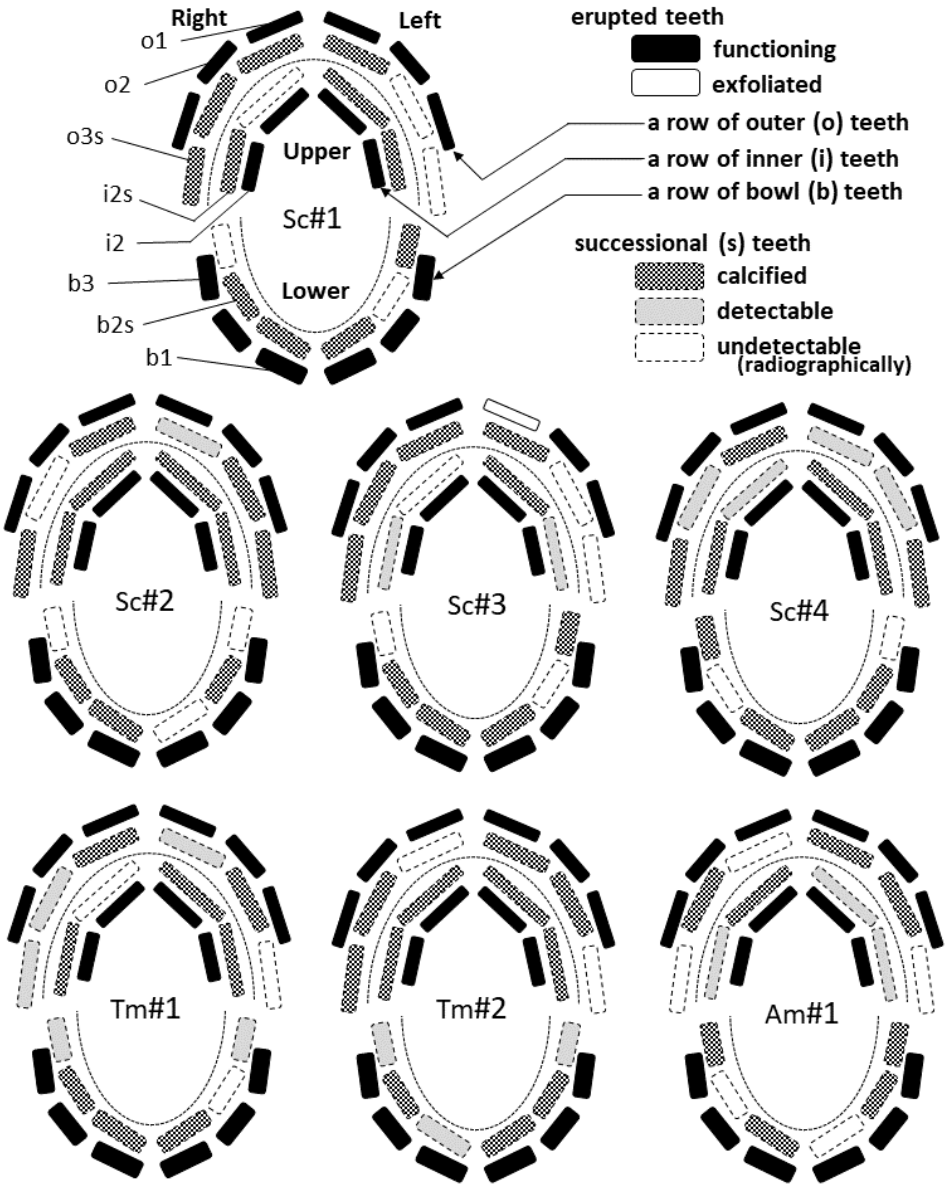

Fig. 6. Schematic summary of the functioning teeth and their successors in 7 specimens examined in this study: *S. cirrhifer* (Sc#1-4), *T. modestus* (Tm#1,2) and *A. monoceros* (Am#1).

Tooth and its position are expressed in the symbols of alphabets and numerals. The development step of successors is evaluated tomographically and coded as explained in the right above.

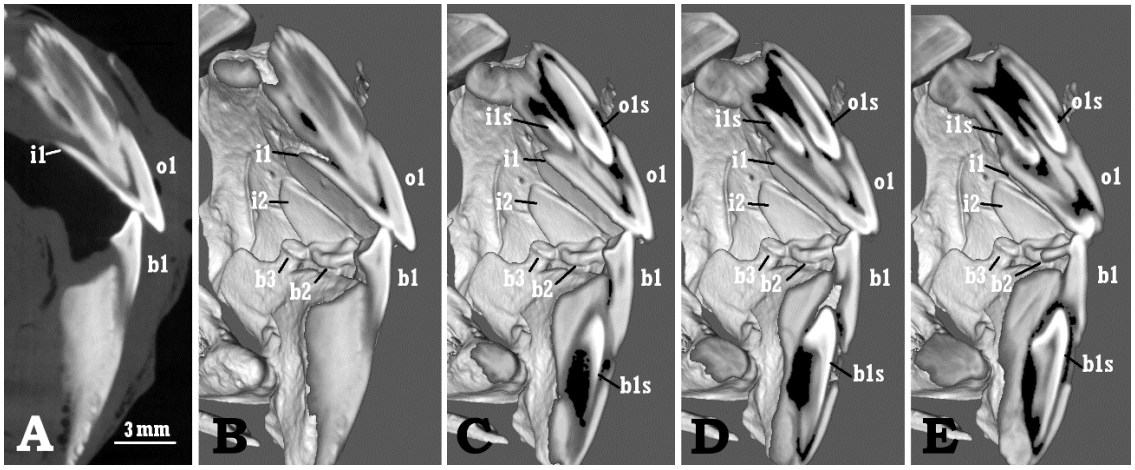

Fig. 7. The occlusal relationship of upper and lower left teeth in *S. cirrhifer* (Sc#1).

The 3D-surface VR images are shown at four sagittal planes from the next to mid-sagittal (B), then sequentially lateral (C, D), and finally to the distal-most of o1 (E). An ordinary tomogram (A) was shown at the next to mid-sagittal plane (identical to B). All images are in the same magnification.

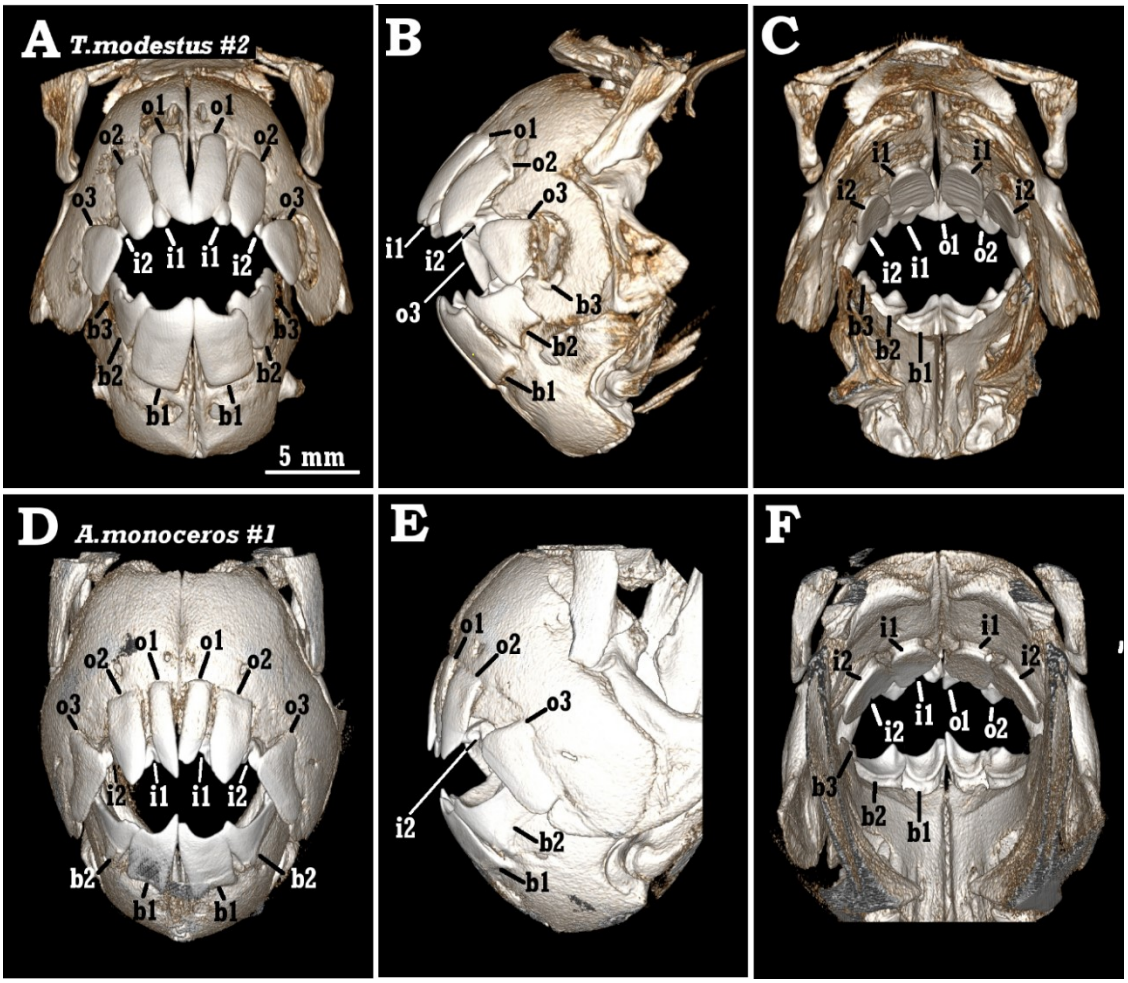

Fig. 8. The teeth-bearing jaws of the specimens of *T. modestus* (Tm#2; A-C) and *A. monoceros* (Am#1; C-F).

The frontal (A, D), lateral (B, E) and caudal (C, F) views of the 3D-VR of jaws are shown in the open positions of jaws. Concerning symbols for tooth and its position, consult "Materials and Methods" and Figure 6. All images are in the same magnification.

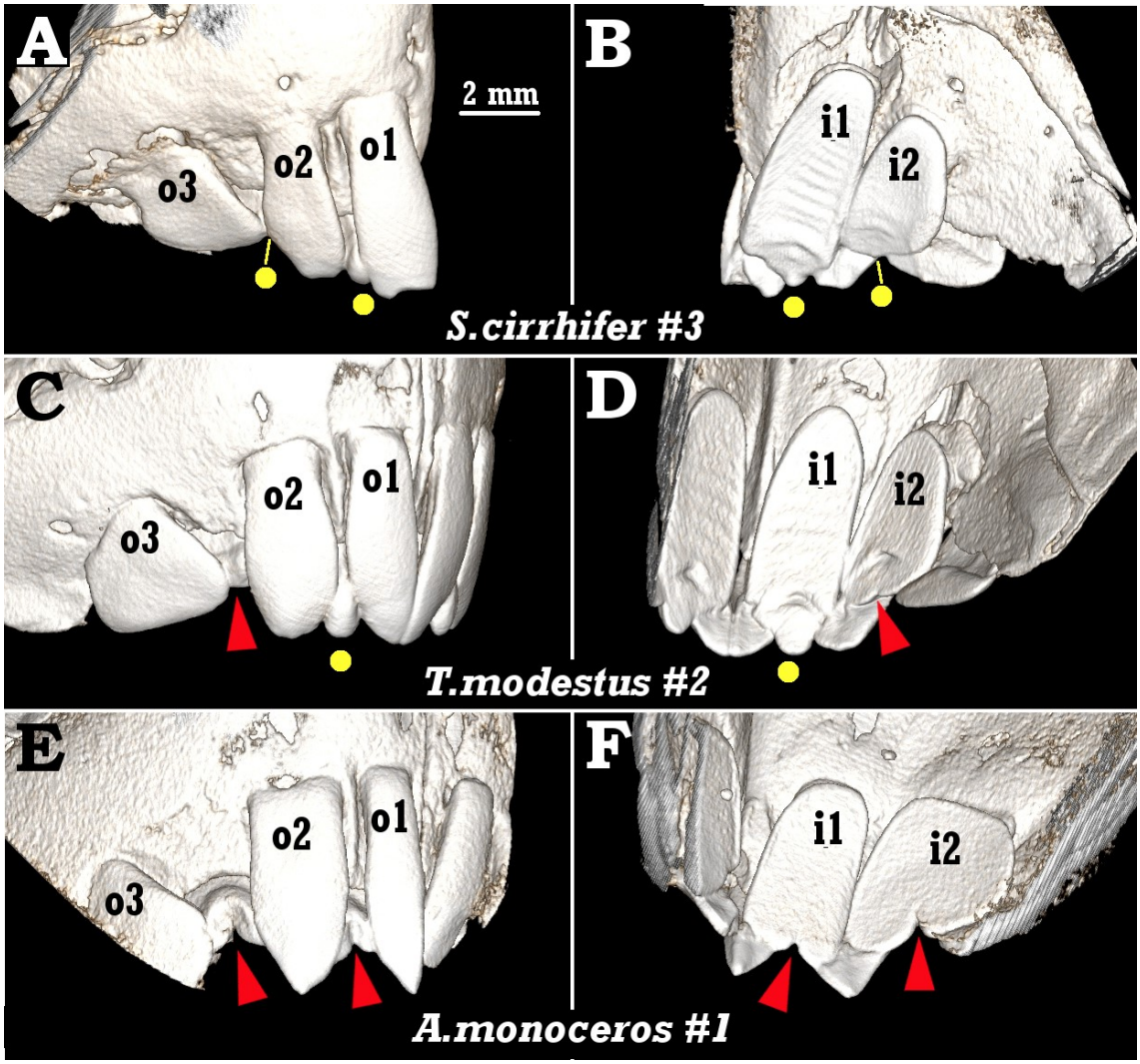

Fig. 9. Dentitions of the right upper jaw in *S. cirrhifer* (A, B), *T. modestus* (C, D) and *A. monoceros* (E, F).

In the labial view (A, C and E), the apices (yellow circles) or the notches (red arrowheads) of i1 and i2 are intercalated with o1-3 teeth. In the lingual view (B, D and F), the entire morphology of i1 and i2 teeth can be seen directly. Each of i1-2 teeth possesses an apex in *S. cirrhifer* (B) and a notch in *A. monoceros* (F). In *T. modestus,* i1 possesses an apex and i2 a notch (D). All images are in the same magnification.

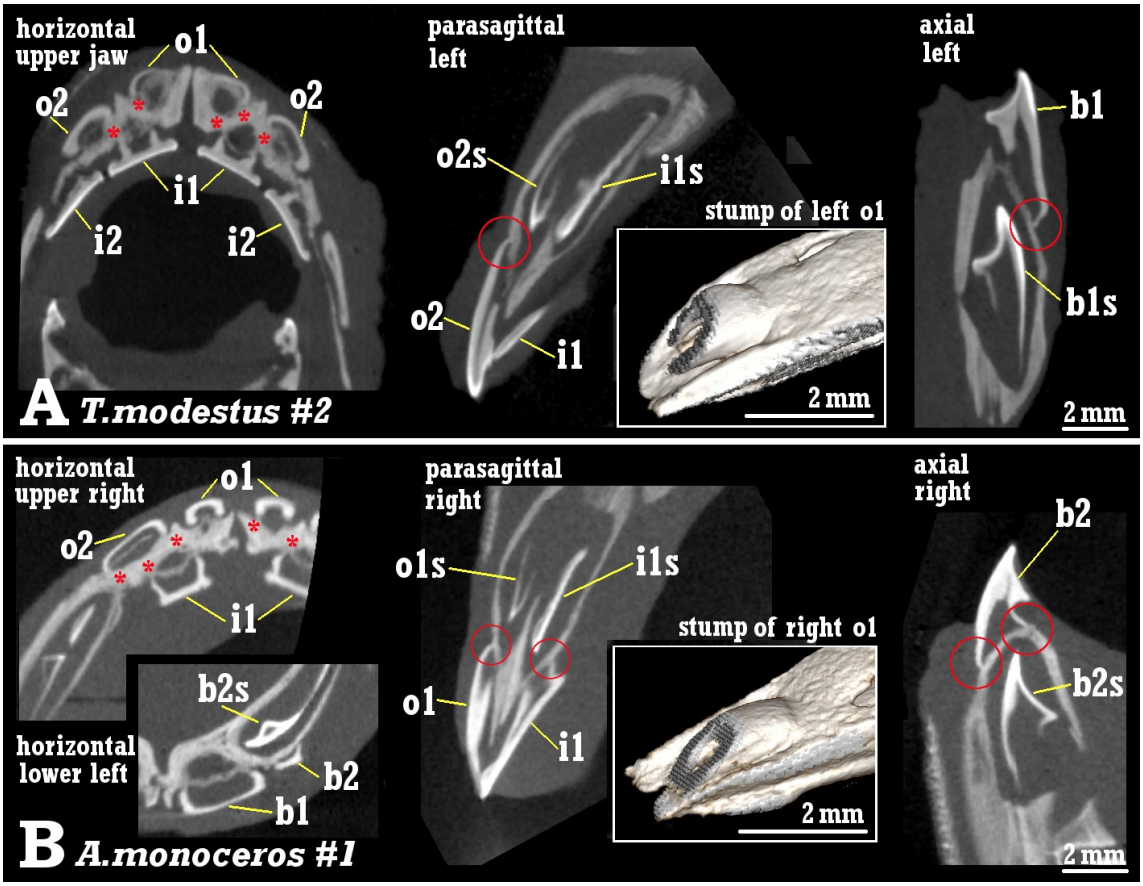

Fig. 10. Tomographical views of the jaws in *T.modestus* (A) and *A. monoceros* (B).

Tomograms focusing on tooth ankylosis to the bone are shown. Bone is labeled with asterisks in red in horizontal tomograms. In other tomograms, sites of tooth ankylosis to the bone are encircled in red. All of the tomograms are in the same magnification. 3D-VR images in the insets of A and B represent a stump of o1 tooth sitting on a shallow depression, but never in a socket.

Table 1. The ratio in the maximum mesiodistal widths in ***S. cirrhifer***, calculated from the width of successional teeth divided by that of predecessors

Specimen & side		Successors		Predecessors*[1]	S/P ratio
		Symbol*[2]	Width (mm) *[3]	Width (mm) *[3]	
Sc#1	left	o1s	2.54	2.25	1.13
Sc#1	right	o2s	2.32	2.22	1.05
Sc#2	right	o1s	2.25	2.01	1.12
Sc#3	left	o1s	2.03	1.91*[4]	1.07
Sc#4	right	o1s	2.50	2.32	1.08
Sc#4	left	i1s	2.75	2.33	1.18
Sc#1	left	b1s	2.22	2.18	1.02
Sc#1	right	b2s	2.45	2.31	1.06
Sc#3	left	b1s	2.66	2.66	1.00
Sc#3	right	b1s	2.80	2.46	1.14
Sc#4	left	b1s	3.18	2.84	1.12

*[1] Erupted and functioning teeth
*[2] Consult Materials & Methods and Figure 6.
*[3] An average of three-time measurements
*[4] Right o1 was measured, since left o1 was exfoliated.

Table 2. The ratio in the maximum mesiodistal widths in ***T. modestus***, calculated from the width of successional teeth divided by that of predecessors

Specimen & side		Successors		Predecessors	S/P ratio
		Symbol	Width (mm)	Width (mm)	
Tm#1	right	o2s	2.25	2.07	1.09
Tm#1	left	i1s	2.54	2.29	1.11
Tm#2	left	i1s	2.64	2.41	1.09
Tm#2	right	i1s	2.50	2.42	1.03
Tm#1	left	b1s	2.97	2.72	1.09
Tm#1	right	b1s	2.96	2.33	1.27
Tm#2	left	b1s	3.34	2.98	1.12

Table 3. The ratio in the maximum mesiodistal widths in ***A. monoceros***, calculated from the width of successional teeth divided by that of predecessors

Specimen & side		Successors		Predecessors	S/P ratio
		Symbol	Width (mm)	Width (mm)	
Am#1	left	o1s	1.44	1.29	1.12
Am#1	left	o2s	2.75	2.35	1.17
Am#1	right	o2s	2.72	2.29	1.19
Am#1	left	b2s	3.34	3.17	1.05